https://doi.org/10.2352/ISSN.2169-4451.2018.34.215

Direct-to-shape: Increasing the throw distance

***Renzo Trip*[1], *Nick Jackson*[1], *Felix Steinchen*[2], *Volker Till*[2], *Werner Zapka*[1]**
[1] ***Xaar PLC, 316 Cambridge Science Park, Milton Rd, CB4 0XR Cambridge, UK***
[2] ***Till GmbH, Siemensstr. 21, 65779 Kelkheim, Germany***

Abstract

Direct-to-shape printing demands a high drop placement accuracy, such that the drop placement is still acceptable at larger throw distances ($>1\,\mathrm{mm}$). In this study, the influence of the nozzle shape on the drop placement accuracy has been investigated. Experiments were conducted employing a series of prototype Xaar 126 printheads fitted with a silicon nozzle plate, with various nozzle taper angles. The results presented in this study show that a larger nozzle taper angle improves the drop placement accuracy; that is, when the printhead is operated at a drive voltage required to have a drop velocity of $6\,\mathrm{m/s}$. The required drive voltage is reduced due to the increased nozzle efficiency associated with a larger nozzle taper angle. A lower drive voltage is likely to be the underlying reason for a smaller drop-to-drop velocity variation, which in turn results in an improved drop placement accuracy. An even better drop placement accuracy is obtained when the drive voltage is increased to give a larger than typical drop velocity (of upto $10.3\,\mathrm{m/s}$), but this also causes the formation of satellite drops reducing the overal print quality.

Introduction

By Direct-to-shape (DTS) we mean digital inkjet printing directly onto packaging such as cans, bottles, sleeves, and other shaped containers. DTS offers various benefits over the traditional use of labels. For example, DTS eliminates the lead time for alternative designs, and also reduces the amount of waste [1]. Furthermore, the non-contact nature of DTS offers a solution to the difficulties that arise when applying labels to bottles having increasingly thinner walls [2].

Printing directly onto curved surfaces will often involve a larger throw distance compared to the typical throw distance of about $\lesssim 1$ mm common for inkjet applications on flat substrates. For example, printing on glass and PET containers requires a throw distance of 5 mm [3]. A larger throw distance decreases the drop placement accuracy, and may therefore result in poor print quality.

The drop placement accuracy can be improved by increasing the drop velocity. If the window of operation permits, a higher drop velocity can simply be obtained by increasing the drive voltage. Alternatively, the nozzle efficiency can be improved to increase the drop velocity [4], for example by increasing the nozzle taper angle [5]. Besides the drop velocity, the nozzle shape can also affect the drop directionality [4]. Furthermore, the stiffness of the nozzle plate, related to the material it is made of, does also effect the drop velocity [6].

In the present study, the influence of the nozzle taper angle on the drop velocity and the drop placement accuracy is investigated experimentally. A standard Xaar 126 printhead design is modified by fitting various silicon nozzle plates with different nozzle taper angles. The results are compared to the standard printhead fitted with a Upilex nozzle plate. The drop ejection performance is investigated by means of a delayed double-flash technique. In addition, the drop placement accuracy is assessed by analysing print samples made at increasing throw distances.

Experimental details

The Xaar 126-35 printhead is a 17 mm piezoelectric drop-on-demand printhead of the end-shooter type, with 126 active nozzles on a single row. The ex-situ nozzle plate makes this printhead particularly suitable for the study presented here. The printhead is operated at a fixed drive voltage. All experiments are carried out using Agfa XES test fluid at room temperature.

In this study, 4 printheads are considered which are listed in Table 1. Besides the standard Xaar 126 (`Xaar 126-35`) printhead with a Upilex nozzle plate, three modified versions of the same printhead with silicon nozzle plates mounted are investigated. The only difference between these three modified printheads is the nozzle taper angle of 8°, 15°, and 21°, respectively. The printhead with a 21° taper angle will be operated at two different drive voltages (15V and 20V), and is therefore listed twice.

The nozzle shape is best described by a truncated cone with a cylindrical exit orifice. The nozzle exit diameter is 25 μm for all investigated printheads, and hence, only the nozzle inlet diameter is altered to achieve different taper angles of the same nozzle plate thickness/nozzle length ratio.

Table 1: Overview of printheads

Ref.	Material	Taper
`Xaar 126-35`	Upilex (PI)	15°
`Si8°20V`	Silicon (Si)	8°
`Si16°17V`	Silicon (Si)	16°
`Si21°15V`	Silicon (Si)	21°
`Si21°20V`	Silicon (Si)	21°

First, the drop ejection performance is investigated using a delayed double-exposure spark-flash technique on a microscope rig. A simple all nozzles firing, 3-line image was printed and three parameters were recorded; 1) the drive voltage required for $6\,\mathrm{m/s}$ drop velocity at 1 mm, 2) the maximum drop velocity before satellites are visible at 1 mm throw distance, and 3) the drive voltage for this satellite threshold drop velocity. In addition, the number of satellites and the directionality of the ligature of the drops are investigated using this measurement technique.

Second, print tests are conducted at a print rig which has a 2-dimensional translation stage. The printhead mount, which allows for angle correction, is attached to a micrometer translation stage which is used to vary the throw distance. This experimental setup is shown in figure 1. The head is gravity fed, where the ink reservoir is kept at an underpressure relative to the atmospheric pressure to prevent leakage when idle. The coordinate system is orientated such that the print and cross-print direction align with the y- and x-axis, respectively. Note that the drop velocity U is smaller than zero and is orientated with the z-direction.

For these print tests, every third nozzle is used, which results in 42 printed nozzles. The prints are carried out in a bi-

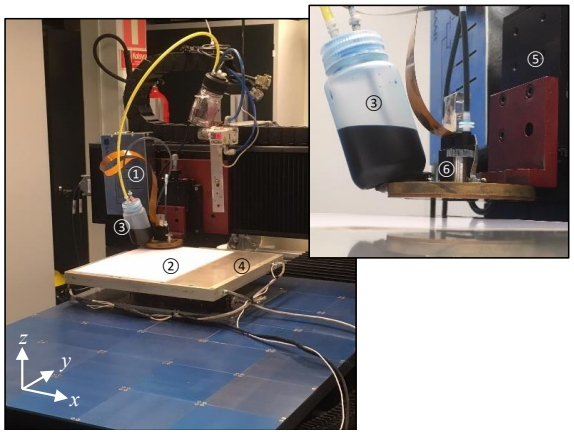

Figure 1. *ACERLINK printrig with: 1) Xaar 126 (HPC), 2) substrate, 3) ink reservoir, 4) 2D-translating stage, 5) micrometer translator, 6) printhead.*

directional mode, which means that the image is printed twice, once with the table moving in the positive y-direction and once with the table moving in the negative y-direction. The print speed is equal to 1 m/s for all tests, and the substrate is *Epson Premium Glossy* photo paper. The image is 10 pixels long, so two blocks of 10×42 drops are printed for each configuration of printhead, drive voltage and throw distance.

The drop placement is measured with a Mitutoyo Quick Vision ELF (QV7) 3D CNC vision measuring machine. The Mitutoyo has a resolution of 0.1 µm and an accuracy of 2.7 µm. The Mitutoyo provides the coordinates of all 10×42 drops, relative to a chosen origin. The drops printed with the first and last nozzle are neglected, as well as the first three drops printed with each nozzle, resulting in 7×40 data points. The final result consists of two matrices containing x- and y-coordinates of drops which are normally distributed around the ideal rectangular grid aimed for. The difference between the target coordinates and the measured coordinates will be referred to as Δx and Δy.

Drop velocity

One factor that determines the drop placement accuracy in the print direction is the drop velocity and the related flight time. That is, a larger drop velocity leads to a reduction of the time in flight of the drop. As a result, the variation of the drop placement in the print direction is reduced. The drop velocity U as function of time t can be derived by considering the drag force acting on an ink drop.

The drag force F_{Drag} acting on a small spherical object, such as an ink drop, is referred to as Stokes' drag, which is given by:

$$F_{\text{Drag}} = -6\pi\mu RU \ , \tag{1}$$

with μ the dynamic viscosity of the surrounding medium, and R the radius of the drop. The gravitational force, which is also acting on a drop in flight, can be shown to be negligible in the case of an ink drop. Therefore, according to Newton's second law, the velocity U of the drop is given by:

$$\frac{dU}{dt} = -AU \ , \tag{2}$$

with $A = 6\pi\mu R/m$, in which m is the mass of the ink drop:

$$m = V_{\text{drop}}\rho_{\text{ink}} = \frac{4}{3}\pi R^3 \rho_{\text{ink}} \ , \tag{3}$$

where V_{drop} is the drop volume and ρ_{ink} the density of the ink. The solution of equation 2, a first order linear ordinary differential equation with the initial drop velocity $U(0) = -U_0$, is given by:

$$U(t) = -U_0 \exp[-At] \ . \tag{4}$$

Then, the distance of the drop $z(t)$ to the substrate is found by integration of $U = dz/dt$ (equation 4):

$$z(t) = \frac{U_0}{A}\exp[-At] - \frac{U_0}{A} + z_{\text{ph}} \ . \tag{5}$$

The integration constant is solved for using the initial distance of the drop to the substrate, $z(0) = z_{\text{ph}}$, where z_{ph} is referred to as 'throw distance'.

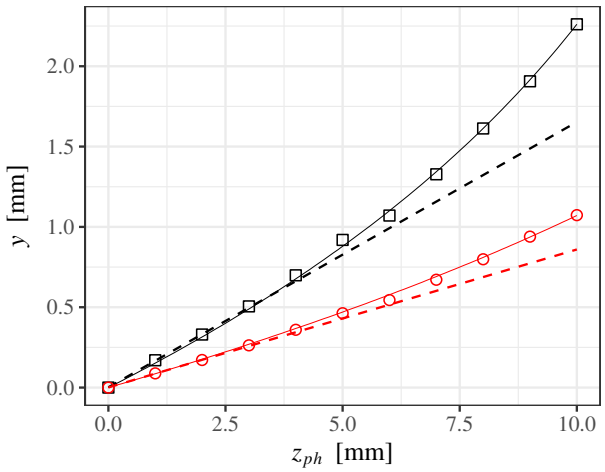

Figure 2. *The distance y traveled by the substrate during the flight time of a drop required to overcome the throw distance z_{ph}. Two cases, Si21° 15V (□) and Si21° 20V (○) are shown in black and red, respectively. Experimental data is marked with open symbols and a fit based on equation 5 is presented with a solid line. A linear fit through the first three points is shown with a dashed line.*

The relation given in equation 5 agrees well with data obtained experimentallly, see figure 2. Instead of the time t, the distance y travelled by the substrate during the flight time of a drop is shown. The distance y is obtained by taking the difference between the average y-coordinate of all 7×40 drops printed while moving the substrate in one direction and the average y-coordinate of all 7×40 drops printed while moving the substrate in the opposite direction.

Table 2: Drop properties

Ref.	Drive Volt. [V]	U_0 [m/s]
Xaar 126-35	NA	4.3
Si8°(20V)	20	5.5
Si16°(17V)	17	6.0
Si21°(15V)	15	5.9
Si21°(20V)	20	10.3

To obtain the fit based on equation 5, delineated with a solid line in figure 2, the initial drop velocity U_0 is determined first. It is evident from figure 2, that y is approximately proportional to z up to at least $z = 3$ mm for the cases studied here. The proportionality constant, obtained by a linear fit through data points in the range $z = 0\,\text{mm} - 3\,\text{mm}$, is equal to the ratio of the print speed and the initial drop velocity U_0. With a print speed of 1 m/s, U_0

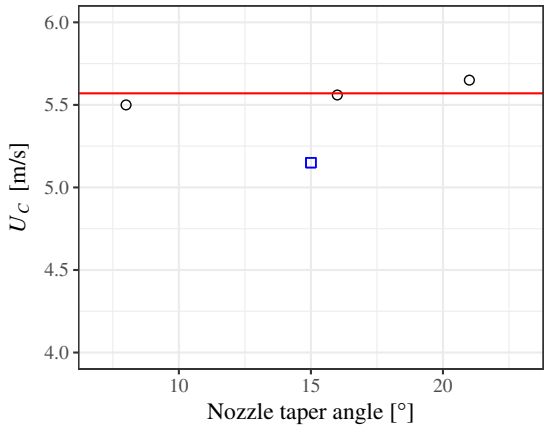

Figure 3. *The critical drop velocity U_C at which satellites are observed at a throw distance $z_{ph} = 1$ mm, as function of the nozzle taper angle. Printheads with a silicon nozzle plate are marked with a black circle (○), and the average for all nozzle taper angles is shown with a red solid line. The `Xaar 126-35` printhead is marked with a blue square (□).*

is simply equal to the reciprocal of the proportionality constant. The U_0 values obtained by this method are listed in Table 2.

The drive voltage, listed in Table 2, is chosen to be the maximum printhead operation voltage before which satellites are visible at $z_{ph} = 1$ mm, which is judged from the spark-flash experiments. The drop velocity at 1mm throw distance at the drive voltage obtained in this way is shown in figure 3. The maximum drop velocity before satellite formation is lower for the `Xaar 126-35`- printhead, but does not change significantly with increase of taper angle for the printheads with a silicon nozzle plate.

The drive voltage of the printhead required to obtain the critical velocity U_C does significantly decrease with increasing nozzle taper angle within the investigated range, as can be observed from figure 4. The `Xaar 126-35`-printhead with a Upilex nozzle plate aligns well with the silicon nozzles.

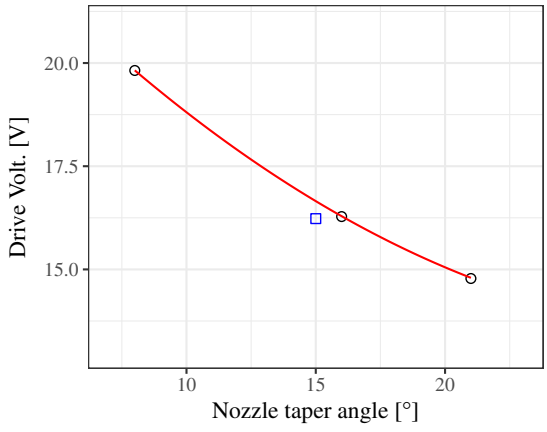

Figure 4. *Printhead drive voltage required to obtain a drop velocity $U = 6$ m/s at a throw distance $z_{ph} = 1$ mm as function of the nozzle taper angle. Printheads with a silicon nozzle plate are marked with a black circle (○), and the trend with increasing nozzle taper angle is emphasized with a red solid line. The `Xaar 126-35` printhead is marked with a blue square (□).*

The reduced drive voltage required to obtain the desired initial drop velocity has the additional advantage of a lower cross talk. During the spark-flash measurements of the printhead with

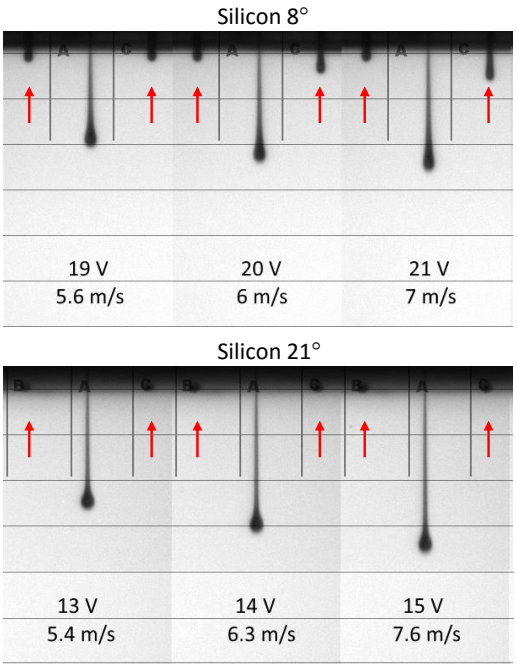

Figure 5. *Series of spark-flash images of `Si8° (20V)` and `Si21° (15V)` at various drive voltages, with arrows indicating the protrusions at the neighbouring nozzles.*

an 8° nozzle taper angle it is noticed that the neighbouring nozzle meniscus is protruding from the nozzle to an extent that it appears to be close to detaching. By comparison, the meniscus of the printhead with a nozzle taper angle of 21° taper heads protrudes significantly less, as is shown in figure 5. The protrusion of ink from neighbouring nozzles is associated with flooding/pooling and can therefore affect the drop placement accuracy in a negative manner.

Additional observations from the spark-flash measurements, not shown here, show the drop volume to be consistent for all printheads examined here, being 30 pL. The number of satellites does not increase with nozzle taper angle, but is elevated for the printhead with a Upilex nozzle plate. This can be explained by the larger ligature length observed in this case, compared to the printheads with a silicon nozzle plate. A final, important, observation is that the spark-flash measurements do not show an effect of the nozzle taper angle or nozzle plate material on the drop ejection angle deviation.

Drop placement accuracy

In this section, the drop placement accuracy will be discussed. An obvious measure for the drop placement accuracy is the standard deviation of the placement error distribution. We will first investigate whether this is indeed a proper metric.

In absence of systematic errors, the drop placement should be randomly distributed around the origin. In figure 6 the scatter plot of the drop placement errors is shown, which also proves that Δy and Δx are independent of each other. The histograms of the placement errors Δy and Δx are shown in figure 7 and figure 8, respectively. The standard deviation of Δy and Δx, σ_y and σ_x, respectively, are also deduced and used to calculate the normal distribution shown. We can conclude that the data is normally distributed and that the standard deviation is a proper metric to quantify the drop placement accuracy.

In figure 9, the drop placement accuracy σ_y in the print di-

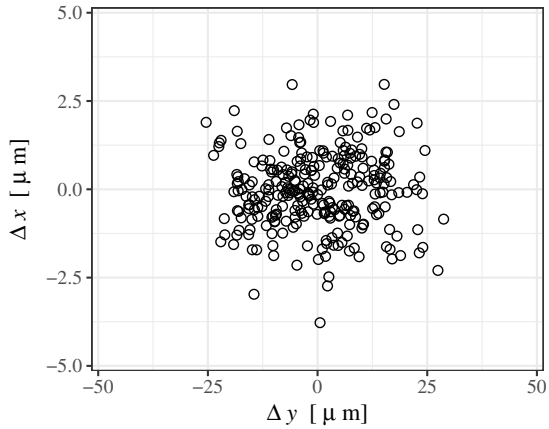

Figure 6. *Scatter plot of the placement errors in print (Δy) and cross-print (Δx) direction (Si21° (15V), $z_{ph} = 5$ mm).*

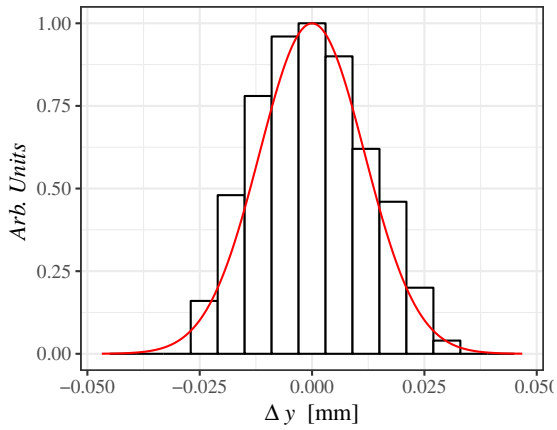

Figure 7. *Histogram of the placement error Δy (print direction). The number of counts in each bin is normalized with the total number of counts. The normal distribution curve based on the standard deviation σ_y is also shown with a red solid line.*

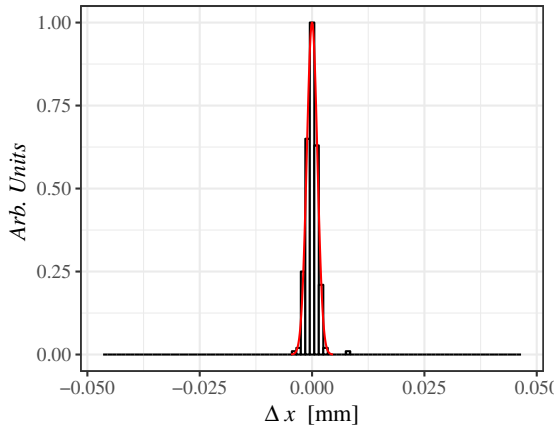

Figure 8. *Histogram of the placement error Δx (cross-print direction). The number of counts in each bin is normalized with the total number of counts. The normal distribution curve based on the standard deviation σ_x is also shown with a red solid line.*

rection is shown. If one considers only those cases for which the nozzle plate is made of silicon (Si...°(...V)), it can be concluded that an increase of nozzle taper angle leads to a considerable increase of the drop placement accuracy, indicated by a

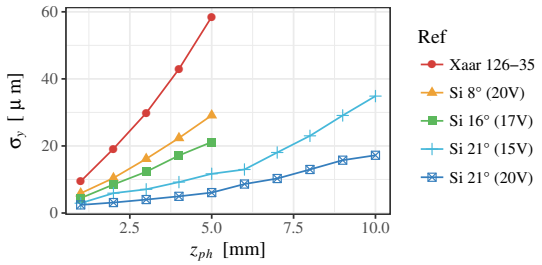

Figure 9. *The drop placement accuracy σ_y in the print direction as function of the throw distance z_{ph}*

decrease of σ_y. σ_y increases roughly linearly with throw distance up to $z \approx 5$ mm. For both cases for which data at higher throw distances is obtained, an increased growth of σ_y is observed. Referring to equation 4 and figure 2, this can be explained by the fact that the effect of drag becomes visible for $z > 5$ mm. In other words, the drop placement accuracy follows the same trend as the time of flight of the drop. An increase of U_0 leads to a further decrease of the drop placement accuracy, which can be concluded when comparing Si21°(15V) to Si21°(20V), were the latter is operated at a higher drive voltage and thus larger initial drop velocity.

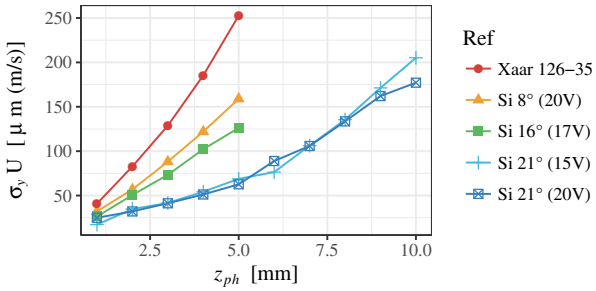

Figure 10. *The drop placement accuracy σ_y in the print direction multiplied by U_{Drop} as function of the throw distance z_{ph}.*

By assuming that σ_y is inversely proportional to U_0, we can exclude the effect of U_0 by multiplying σ_y with U_0. The result is shown in figure 10. The independence of U_0 is clearly evidenced by the close agreement of Si21°(15V) and Si21°(20V). This suggest that $\sigma_y U_0$ gives a measure for the drop placement accuracy for a combination of nozzle plate material and nozzle taper angle. A silicon nozzle plate gives a better drop placement accuracy than a Upilex nozzle plate. Also, an increase of the nozzle taper angle leads to an improved drop placement accuracy in case of a silicon nozzle plate.

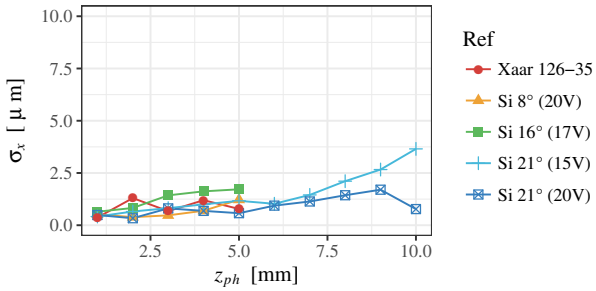

Figure 11. *The drop placement accuracy σ_x in the cross-print direction as function of the throw distance z_{ph}.*

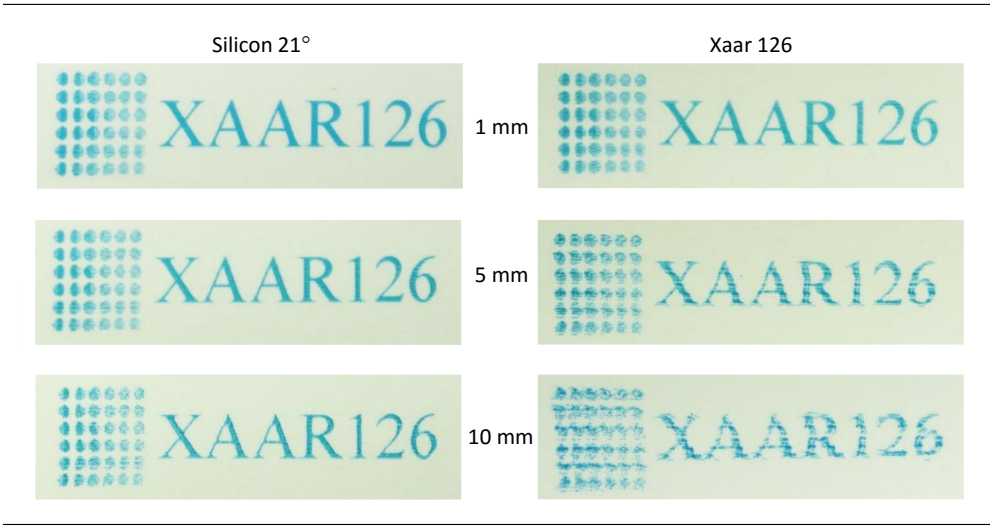

Figure 12. *Example of improved print quality at increased throw distance*

In order to distinguish between the placement error due to a drop-to-drop variation in U_0 and the drop ejection angle deviation, the placement error in the cross-print direction is considered. Thereby we assume that the nozzle is axisymmetric. In figure 11 the drop placement accuracy, expressed in terms of the standard deviation of the placement error, in the cross-print direction is shown as function of the throw distance z_{ph}. It should be mentioned that the placement error in the cross-print direction is of the same order of magnitude as the accuracy of the Mitutoyo. This may explain why there is no clear trend shown. The drop placement accuracy in the cross-print direction is very good for all cases studied here. This leads to the conclusion that the improved drop placement accuracy in the print direction with increased nozzle taper angle is mainly due to a reduced drop-to-drop variation in the initial drop velocity. If a reduced drop ejection angle deviation with increased nozzle taper angle would be the main reason, a clear trend would have been shown in figure 11 as well.

To visualize the impact of an improved drop placement accuracy on an actual print out a test image is produced with both the `Si21°(15V)` and `Xaar 126-35` printhead, at various throw distances. Photographs of the different prints are shown in figure 12. The print speed is $0.2\,\mathrm{m/s}$ in this case. The print quality is clearly better for `Si21°15V` compared to the standard `Xaar 126-35`, most profoundly so at $z_{ph} = 10$ mm.

Discussion and Conclusion

The drop placement accuracy is investigated for four different printheads, the difference being the nozzle plate material and the nozzle taper angle.

Analysis of spark-flash measurements shows that the nozzle efficiency increases with an increase of the nozzle taper angle, independent of the nozzle plate being made of Upilex or silicon. The improved nozzle efficiency allows for a higher drop velocity within the range of operating voltages. However, the critical drop velocity above which satellites are distinguished at 1 mm does not increase significantly with nozzle taper angle over the range investigated. The printheads with a silicon nozzle plate do have a larger critical drop velocity compared to the printhead with a Upilex nozzle plate. Due to the improved nozzle efficiency associated with a larger taper angle, the required drive voltage to obtain the critical drop velocity is 25% lower for the largest nozzle taper angle compared to the smallest nozzle taper angle. As a result, there is less cross talk and the protrusions from neighbouring nozzles and the associated problems of flooding/pooling are reduced.

From the results of the standard deviation of the drop placement error in the print direction it can be concluded that an increase of the nozzle taper angle leads to an improved drop placement accuracy. The best drop placement accuracy is found for a Silicon nozzle plate with a nozzle taper angle of 21°. The standard Xaar 126-35 printhead with a Upilex nozzle plate has a larger placement error. The improved drop placement accuracy is even obtained without an increase of the initial drop velocity.

The drop placement error in the cross-print direction is a factor of ten smaller than the drop placement error in the print direction. This suggest that the drop placement error is primarily the result of the drop-to-drop variation in the initial drop velocity. In other words, an increase of the nozzle taper angle leads to a reduction of the drop-to-drop variation in the initial drop velocity. No change in drop ejection nozzle deviation is observed. The fact that Upilex is not as good, even for comparable nozzle taper angle, suggest that the nozzle plate material does have an influence on the drop-to-drop variation of the initial drop velocity as well.

References

[1] Zapka, W., Handbook of Industrial Inkjet Printing - A full System Approach (Vol. 2), Wiley, Weinheim, Germany, 2017, pg. 787.

[2] Zapka, W., Handbook of Industrial Inkjet Printing - A full System Approach (Vol. 2), Wiley, Weinheim, Germany, 2017, pg. 799.

[3] Till, V., Inkjet Decoration of curved surfaces at high capacities - Challenges and successful implementation, IMI (2013).

[4] Levanoni, M., Study of fluid flow through scaled-up ink jet nozzles, IBM J. Res. Develop.,

[5] Takeuchi, Y., Takeuchi, H., Komatsu, K., Nishi, S., Improvement of drive energy efficiency in a shear mode piezo-inkjet head, Hp Company Report (1998).

[6] Sangplung, S. and Liburdy, J.A., Droplet formation under the effect of a flexible nozzle plate, J. Colloid Interface Sci., Vol. 21, pg. 56 (1977).

Author Biography

Renzo Trip obtained a MSc. Degree in Applied Physics at Delft University of Technology (Delft, The Netherlands). The focus on Fluid

Mechanics during the last year of the study lead to a post graduate position in the Fluid Physics Laboratory, part of the Mechanics department of KTH Royal Institute of Technology (Stockholm, Sweden). Thereafter, Renzo joined Xaar plc (Stockholm office, Sweden) in the function of development engineer as part of the Advanced Application Technology group.